The influence of dichroic beam splitter on the airborne multiband co-aperture optical system*

XING Zhen-chong (邢振冲)[1,2], **HONG Yong-feng** (洪永丰)[1], **and ZHANG Bao** (张葆)[1]**

1. Changchun Institute of Optics, Fine Mechanics and Physics, Chinese Academy of Sciences, Changchun 130033, China

2. University of Chinese Academy of Sciences, Beijing 100059, China

(Received 29 December 2017; Revised 23 March 2018)

The multiband co-aperture optical system with compact structure can achieve full and effective integration of multi-source intelligence information, which is one of the development direction of the optical system. Dichroic beam splitter is a vital optical component to make several systems with different bands share one aperture. The effect of the dichroic beam splitter on the multiband co-aperture optical system is analyzed by matrix optics method and primary aberration theory. The results indicate that the reflection angle of the dichroic beam splitter as a reflector changes imaging direction, and the wedge angle of the dichroic beam splitter as a transmission component increases some aberrations.

Document code: A **Article ID:** 1673-1905(2018)04-0252-5

DOI https://doi.org/10.1007/s11801-018-7273-0

In modern warfare, the next generation stealth fighter becomes a multifunctional system with stealth, aerobatic maneuver and supersonic speed. Optical-electronical system is the crucial groundwork equipment, which lets the aircraft anticipate and destroy enemy, attack beyond visual range and so on. The multiband co-aperture optical system is the development direction of the aircraft optical-electronical system. Multiband can achieve the all-weather day and night operational capacity. Co-aperture can enhance the operative distance of the aircraft. The global researches in multiband co-aperture optical system have achieved certain results[1-4], such as the electro-optical targeting system whose work wavelengths cover infrared light, visible light and laser placed on the F35. The infrared system, visible system and laser system share one aperture, and dichroic beam splitters split lights and lead each band radiate to the respective detectors[1-9].

However, the present researches about multiband co-aperture optical system at home and abroad focus on the optical designs of the system with the shared aperture and the technology of beam splitters[10-14], and there are few researches penetrate into the influence of dichroic beam splitter on the multiband co-aperture optical system.

In the light path, dichroic beam splitters affect the imaging direction and image quality as a reflector and a transmission component. The reflection angle and wedge angle of the dichroic beam splitter are influenced.

The dichroic beam splitters are designed by their manufacturers to transmit specific wavelengths of light and reflect the other wavelengths of light. In the subsystems of multiband co-aperture optical system, the dichroic beam splitter plays different roles. When the dichroic beam splitter is a reflector, the effect of reflection angle on the image is mainly analyzed. It is the transformation of coordinates that takes place in the reflection transmission of light. Therefore, matrix optics can be used to express coordinate transformation matrix and estimate the positions of image. The relation of coordinate transform in a reflector can be expressed as

$$\begin{bmatrix} x' \\ y' \\ z' \end{bmatrix} = \boldsymbol{M} \begin{bmatrix} x \\ y \\ z \end{bmatrix}, \tag{1}$$

where $[x, y, z]$ is coordinate values of the incident ray, $[x', y', z']$ is coordinate values of the reflect ray, and $\boldsymbol{M}$ is coordinate transform matrix among the reflection. According to the matrix optics[15], $\boldsymbol{M}$ can be shown as

$$\boldsymbol{M} = \begin{bmatrix} \cos^2\alpha + \sin^2\alpha\cos\theta & (1-\cos\theta)\cos\alpha\cos\beta - \sin\theta\cos\gamma & (1-\cos\theta)\cos\alpha\cos\gamma + \sin\theta\cos\beta \\ (1-\cos\theta)\cos\alpha\cos\beta + \sin\theta\cos\gamma & \cos^2\beta + \sin^2\beta\cos\theta & (1-\cos\theta)\cos\beta\cos\gamma - \sin\theta\cos\alpha \\ (1-\cos\theta)\cos\alpha\cos\gamma - \sin\theta\cos\beta & (1-\cos\theta)\cos\beta\cos\gamma + \sin\theta\cos\alpha & \cos^2\gamma + \sin^2\gamma\cos\theta \end{bmatrix}, \tag{2}$$

* This work has been supported by the Major Innovation Project of Changchun Institute of Optics, Fine Mechanics and Physics (No.Y3CX1SS14C).

** E-mail: zhangb@ciomp.ac.cn

where α, β, γ are the angles between $\boldsymbol{n}$ and x, y, z axis, respectively. After $[x, y, z]$ is rotated θ around $\boldsymbol{n}$, $[x', y', z']$ is the new location. Reflection ray can be the equation of the ray that incident ray rotated 180° around normal $\boldsymbol{n}$. Therefore, it can be obtained by substituting θ=180°into Eq.(2) that

$$\boldsymbol{M}_R=\begin{bmatrix}\cos 2\alpha & 2\cos\alpha\cos\beta & 2\cos\alpha\cos\gamma\\ 2\cos\alpha\cos\beta & \cos 2\beta & 2\cos\beta\cos\gamma\\ 2\cos\alpha\cos\gamma & 2\cos\beta\cos\gamma & \cos 2\gamma\end{bmatrix}. \quad (3)$$

In the multiband co-aperture optical system, there are many dichroic beam splitters. Incident ray reflected by several dichroic beam splitters can be expressed as

$$L'=\boldsymbol{M}_1\boldsymbol{M}_2\boldsymbol{M}_3\ldots\boldsymbol{M}_N(-1)^N L, \quad (4)$$

where L' is the incident ray, L is the reflection ray, M_1, M_2, M_3,…, M_N are reflection matrixes, and N is the number of dichroic beam splitters as the reflector.

When the light transmits the dichroic beam splitter, the dichroic beam splitter is a parallel plate. In the transmission light path, it is the wedge angle of the dichroic beam splitter that can introduce primary aberrations. The analysis about the relationship between the wedge angle and primary aberrations can offer the guide for optical design.

When the converging light is incident in a parallel plate with wedge angle of ε, the light path is shown in Fig.1.

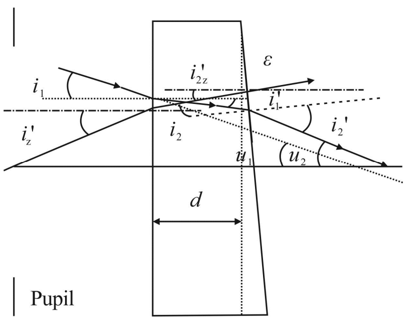

Fig.1 Converging light incident on a parallel plate with a wedge angle

As shown in Fig.1, it can be obtained that

$$i_1'=\frac{i_1}{n}, \quad (5)$$

$$i_2=i_1'+\varepsilon, \quad (6)$$

$$i_2'=ni_2, \quad (7)$$

$$u_2=i_2'-\varepsilon=n(\varepsilon+\frac{u_1}{n})-\varepsilon, \quad (8)$$

$$i_{z2}=\frac{i_z}{n}-\varepsilon. \quad (9)$$

According to the primary aberration theory and Eqs.(5)—(9), Eqs.(10)—(16) can be acquired that

$$\sum_{i=1}^{2}S_{\mathrm{I}}=\varepsilon h_1 n(\varepsilon+\frac{u_1}{n})\left[\varepsilon-n(\varepsilon+\frac{u_1}{n})+\frac{u_1}{n}\right]-h_1u_1(u_1-\frac{u_1}{n})^2, \quad (10)$$

$$\sum_{i=1}^{k}S_{\mathrm{II}}=h_1n(\varepsilon-\frac{i_z}{n})\left[\varepsilon-n(\varepsilon+\frac{u_1}{n})+\frac{u_1}{n}\right]^2-h_1i_z(u_1-\frac{u_1}{n})^2, \quad (11)$$

$$\sum_{i=1}^{k}S_{\mathrm{III}}=h_1i_z^2(\frac{1}{n}-1)(u_1-\frac{u_1}{n})+\frac{\varepsilon h_1n_1(\varepsilon-\frac{i_z}{n})^2\left[\varepsilon-n_1(\varepsilon+\frac{u_1}{n})+\frac{u_1}{n}\right]}{\varepsilon+\frac{u_1}{n}}, \quad (12)$$

$$\sum_{i=1}^{k}S_{IV}=0, \quad (13)$$

$$\sum_{i=1}^{k}S_{\mathrm{V}}=-h_1i_z^3(\frac{1}{n}-1)^2-\frac{\varepsilon h_1n_1(\varepsilon-\frac{i_z}{n})^3\left[\varepsilon-n_1(\varepsilon+\frac{u_1}{n})+\frac{u_1}{n}\right]}{(\varepsilon+\frac{u_1}{n})^2}, \quad (14)$$

$$\sum_{i=1}^{k}C_{\mathrm{I}}=\Delta\frac{dn}{n}n\left[h_1(\varepsilon+\frac{u_1}{n})+\frac{h_1}{u_1}\right], \quad (15)$$

$$\sum_{i=1}^{k}C_{\mathrm{II}}=\Delta\frac{dn}{n}n\left[h_1i_z-h_1(\varepsilon-\frac{u_1}{n})\right]. \quad (16)$$

When the parallel light is incident in a parallel plate with a wedge angle,

$$u_1=0, \quad (17)$$

$$i_1'=i_1=0, \quad (18)$$

$$u_2=i_2'-\varepsilon=n(\varepsilon+\frac{u_1}{n})-\varepsilon=0, \quad (19)$$

$$i_2=\varepsilon, \quad (20)$$

$$i_2'=n\varepsilon, \quad (21)$$

$$h_1=h_2. \quad (22)$$

By substituting Eqs.(17)—(22) into Eqs.(10)—(16), it can be obtained that

$$\sum_{i=1}^{2}S_{\mathrm{I}}=\sum_{i=1}^{k}S_{\mathrm{II}}=\sum_{i=1}^{k}S_{\mathrm{III}}=\sum_{i=1}^{k}S_{\mathrm{IV}}=\sum_{i=1}^{k}S_{\mathrm{V}}=0, \quad (23)$$

$$\sum_{i=1}^{k}C_{\mathrm{I}}=\Delta\frac{dn}{n}n(h_1\varepsilon), \quad (24)$$

$$\sum_{i=1}^{k}C_{\mathrm{II}}=n\Delta\frac{dn}{n}h_1(i_{z2}+i_{z1}). \quad (25)$$

In summary, the dichroic beam splitter which transmits converging light will bring a variety of aberrations, but the dichroic beam splitter which transmits parallel light will bring chromatic aberration only.

The theory above can provide the guiding significance in the optical design process. Fig.2 shows a multiband co-aperture optical system using Cassegrain system, which is a combination of infrared optical system, visible light optical system and laser light path. The optical paths of each band are grouped together by the beam splitter together as shown in Fig.3. On account of volumetric requirement of the airborne optical system, compensation system for the aberrations is not the best choice. We need to take advantage of the characteristics of the aberrations to eliminate or reduce threats. Because the visible system is insensitive to aberrations, aberrations are caused by the dichroic beam splitter, and collimating lens is designed for common optical path of the visible and laser. The infrared system is not sensitive to aberrations, and it can use the method of optical optimization to reduce the impact of the beam splitting.

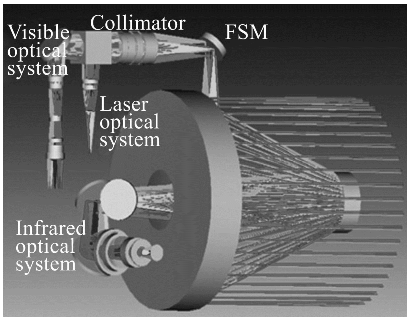

Fig.2 Schematic diagram of multiband co-aperture optical system

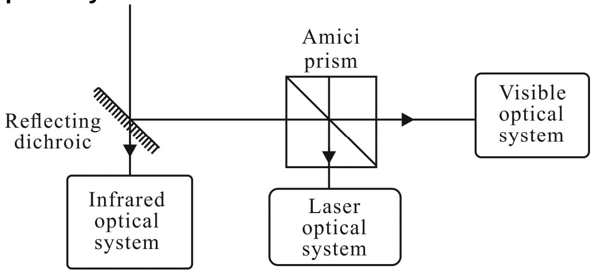

Fig.3 The schematic diagram of beam splitting

In this system, the relative motion of the mirrors causes the image to rotate. Fig.4 shows the spherical coordinate transform of light transmitted by two mirrors.

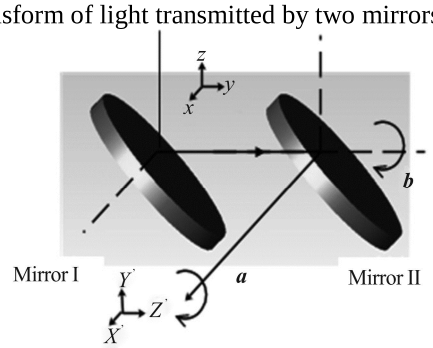

Fig.4 The relative motion of the two mirrors

Assume that mirror I is static and mirror II is rotated relative to mirror I around x axis and y axis. Fig.5 shows the spherical coordinate transform between coordinate system of the incident light and coordinate system of the reflect light through the mirror I and mirror II.

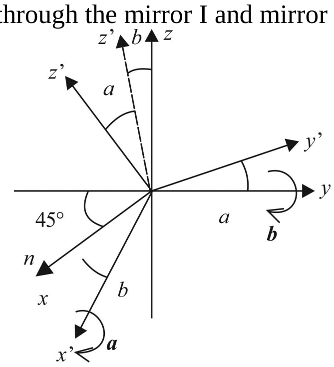

Fig.5 Spherical coordinate transform of the mirror I and mirror II

According to the theory above, the coordinate transform matrix that mirror II rotates a and b around x and y axes can be shown as

$$\boldsymbol{M}=\boldsymbol{M}(\theta=b,\alpha=90^\circ,\ \beta=0,\gamma=90^\circ)\times \boldsymbol{M}(\theta=a,\alpha=0,\ \beta=90^\circ,\gamma=90^\circ)=\begin{bmatrix}\cos b & \sin a\sin b & \sin b\cos a\\ 0 & \cos a & -\sin a\\ -\sin b & \cos b\sin a & \cos b\cos a\end{bmatrix}. \tag{26}$$

Therefore, the normal of the coordinate system of the reflect light can be calculated by

$$\begin{bmatrix}n'_{\mathrm{II}x}\\ n'_{\mathrm{II}y}\\ n'_{\mathrm{II}z}\end{bmatrix}=\boldsymbol{M}\begin{bmatrix}n_{\mathrm{II}x}\\ n_{\mathrm{II}y}\\ n_{\mathrm{II}z}\end{bmatrix}, \tag{27}$$

where [$n_{\mathrm{II}x}$, $n_{\mathrm{II}y}$, $n_{\mathrm{II}z}$] and [$n'_{\mathrm{II}x}$, $n'_{\mathrm{II}y}$, $n'_{\mathrm{II}z}$] are the normal of reflecting surface in mirror II before and after rotating, respectively. The location of mirror II in Fig.4 is taken as the initial location and [$n_{\mathrm{I}x}$, $n_{\mathrm{I}y}$, $n_{\mathrm{I}z}$] is the normal of reflecting surface in mirror I, which is expressed as

$$\begin{bmatrix}n_{\mathrm{I}x}\\ n_{\mathrm{I}y}\\ n_{\mathrm{I}z}\end{bmatrix}=\begin{bmatrix}0\\ \frac{\sqrt{2}}{2}\\ \frac{\sqrt{2}}{2}\end{bmatrix}. \tag{28}$$

On the basis of Eq.(3), because mirror I is stationary, $\boldsymbol{M}$ is shown as

$$\boldsymbol{M}_{\mathrm{RI}}=\begin{bmatrix}-1 & 0 & 0\\ 0 & 0 & 1\\ 0 & 1 & 0\end{bmatrix}. \tag{29}$$

In Fig.4, [$n_{\mathrm{II}x}$, $n_{\mathrm{II}y}$, $n_{\mathrm{II}z}$] can be expressed as

$$\begin{bmatrix}n_{\mathrm{II}x}\\ n_{\mathrm{II}y}\\ n_{\mathrm{II}z}\end{bmatrix}=\begin{bmatrix}0\\ -\frac{\sqrt{2}}{2}\\ -\frac{\sqrt{2}}{2}\end{bmatrix}. \tag{30}$$

By substituting Eq.(30) into Eq.(27), it can be obtained that

$$\begin{bmatrix} n'_{\mathrm{II}x} \\ n'_{\mathrm{II}y} \\ n'_{\mathrm{II}z} \end{bmatrix} = -\frac{\sqrt{2}}{2}\sin\beta(\sin\alpha+\cos\alpha)\boldsymbol{i} + \left(-\frac{\sqrt{2}}{2}\cos\alpha+\frac{\sqrt{2}}{2}\sin\alpha\right)\boldsymbol{j} - \frac{\sqrt{2}}{2}\cos\beta(\sin\alpha+\cos\alpha)\boldsymbol{k}\ , \quad (31)$$

where ***i***, ***j***, ***k*** are unit vectors of the *x*, *y*, *z* axes, respectively. On the basis of Eq.(31), *α*, *β* and *γ* can be shown as

$$\cos\alpha = -\frac{\sqrt{2}}{2}\sin\beta(\sin\alpha+\cos\alpha)\ , \quad (32)$$

$$\cos\beta = \left(-\frac{\sqrt{2}}{2}\cos\alpha+\frac{\sqrt{2}}{2}\sin\alpha\right)\ , \quad (33)$$

$$\cos\gamma = -\frac{\sqrt{2}}{2}\cos\beta(\sin\alpha+\cos\alpha)\ . \quad (34)$$

Therefore, the reflection ray can be expressed as

$$\boldsymbol{L}' = \boldsymbol{M}_{\mathrm{RI}}\boldsymbol{M}_{\mathrm{R}}(\boldsymbol{L})\ . \quad (35)$$

If incident ray $\boldsymbol{L}=[x, y, z]$, $\boldsymbol{L}'=[-z, x, -y]$ which is calculated by Eq.(35) when mirror II rotates 90° around *x* axis. If incident ray $\boldsymbol{L}=[x, y, z]$, $\boldsymbol{L}'=[x, y, z]$ which is calculated by Eq.(35) when mirror II rotates 0° around *x* axis. The relative changing of the image is shown in Fig.6. The image turns 90°. Eq.(35) reflects the relationship between imaging direction and mirror reflection direction. This relationship can not only plan the optical structure, but also provide mathematical evidence for target tracking.

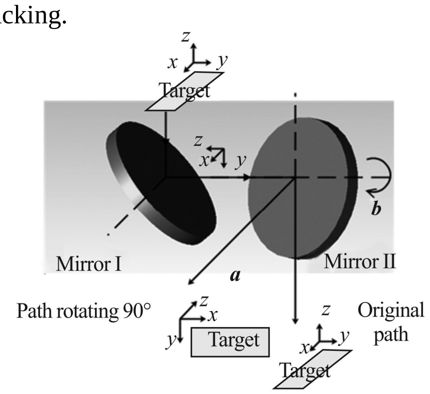

Fig.6 Change of imaging direction

If infrared and visible-light detectors are set up randomly, the images will be shown in Fig.7. This problem can affect the consistency of infrared and visible target tracking[16].

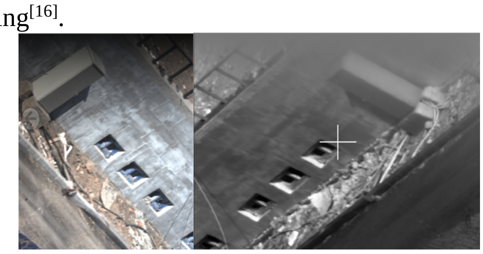

Fig.7 Infrared and visual light images

When dichroic beam splitter is a transmission component as parallel plate for optical system, it can be found that when the parallel plate is set in converging optical path, the wedge angle will bring spherical aberration, coma, astigmatism, curvature of field, distortion and chromatic aberration to the optical system as shown in Fig.8. While, the wedge angle will bring chromatic aberration to the optical system only when the parallel plate is set in parallel optical path as shown in Fig.9. The bigger the wedge angle is, the greater the effect of the optical system on the MTF. If parallel plate is designed in the optical convergence of the optical system, the wedge angle of the plate and the introduction of the aberration itself need to be considered. In addition, we can use Eqs.(10)—(16) to guide the processing of the depth of parallelism of dichroic beam splitter[5].

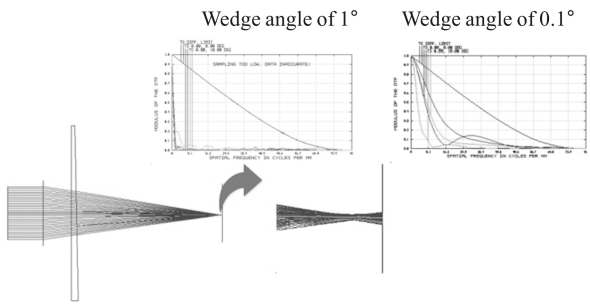

Fig.8 Parallel plate set in converging optical path

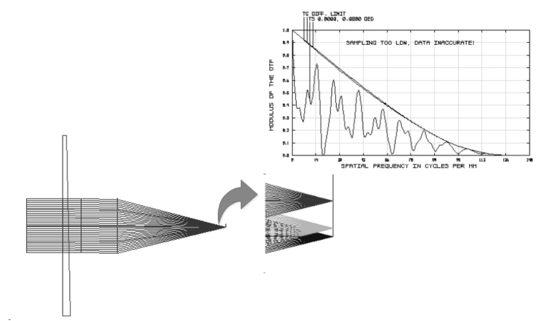

Fig.9 Parallel plate set in parallel optical path

As shown in Fig.10, the dichroic beam splitter set in converging optical path in infrared system is used as transmission flats.

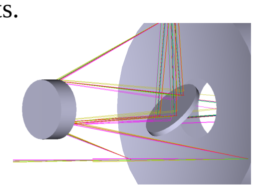

Fig.10 Dichroic beam splitter as parallel plate for infrared system

For the infrared system, we mainly analyze the spherical aberration, coma, astigmatism and distortion. Tab.1 shows the primary aberrations caused by different wedge angles *ε* in the infrared system shown as Fig.2. S1, S2, S3 and S5 are the first, the second, the third and the fifth seidel aberration coefficients, respectively. Tab.2 shows the primary aberrations in the image surface. Comparing Tab.1 with Tab.2, we should choose the reasonable depth of parallelism for the dichroic beam splitter. When the depth of parallelism is 20", the aberrations caused by the dichroic beam splitter have less than 1/2th of aberrations of the system. In addition, during optical design of the infrared system, the value of the dichroic beam splitter aberrations must be considered.

Tab.1 Primary aberrations caused by the wedge angle of the dichroic beam splitter in the infrared system shown as Fig.2

ε	S1	S2	S3	S5
0	0	0	0	0
10"	0.000 54	−0.000 19	0.000 064 2	−0.000 024 7
20"	0.000 75	−0.000 32	0.000 14	−0.000 062 3
30"	0.001 03	−0.000 5	0.000 25	−0.000 13
40"	0.001 38	−0.000 75	0.000 42	−0.000 24

Tab.2 Primary aberrations of the system shown as Fig.2

	S1	S2	S3	S5
System	−0.001 817	−0.000 899	−0.000 764	0.007 432

As shown in Fig.11, the aberrations caused by the dichroic beam splitter do not affect the image quality of the whole system.

(a) (b)

Fig.11 Images of multiband co-aperture optical system: (a) Infrared image; (b) Visible image

Dichroic beam splitter is one of the most important components in a co-aperture optical system. It affects not only the imaging direction but also the imaging quality. Using mathematical methods to analyze the effect of dichroic beam splitter is an essential part of the design of a co-aperture optical system. By establishing a mathematical model, the influence of the dichroic beam splitter in a system is analyzed. Due to the arrangement of the reflected light path, the installation direction of the detector is required to be calculated. At the same time, the analysis results offer the guidance of the dichroic beam splitter and put forward the requirements of reasonable parallelism of the surface of the dichroic beam splitter.

References

[1] Gordeyev Stanislav V, Optical Engineering **52**, 071405 (2013).

[2] Chen Jian, Wang Wei-guo, Liu Ting-xia and Zhang Zhen-dong, Chinese Optics **10**, 777 (2017). (in Chinese)

[3] Li De-dong, Xiao Chu-wan, Feng Xu-yang, Laser & Infrared **47**, 322 (2017). (in Chinese)

[4] Shen Hong-hai, Huang Meng, Li Jia-quan, Liu Jing-hong, Dai Ming and Jia Ping, Chinese Optics **5**, 20 (2012). (in Chinese)

[5] Mu D, Mi S and Mu M, Alimentary Pharmacology & Therapeutics **33**, 286 (2014).

[6] Ming G, Yang C, Liu J and Lv H, Infrared Physics & Technology **64**, 40 (2014).

[7] Lang J, Wang Y, Xiao X, Zhuang X, Wang S, Liu J and Wang J, Optical Engineering **52**, 5008 (2013).

[8] Lasnier C J, Allen S L, Ellis R E, Fenstermacher M E, McLean A G, Meyer W H, Morris K, Seppala L G, Crabtree K and Van Zeeland M A, Review of Scientific Instruments **85**, 11D855 (2014).

[9] Rossi M, Borghi G, Neil I A, Valsecchi G, Zago P and Zocchi F E, Optical Engineering **53**, 031308 (2014).

[10] M. Lombini, A. De Rosa, P. Ciliegi, F. Cortecchia, E. Diolaiti, Mauro Patti, M. Bonaglia, L. Busoni, V. De Caprio, S. Esposito, P. Feautrier, P. Rabou, M. Riva and E. Stadler, Ground-based and Airborne Instrumentation for Astronomy VI, International Society for Optics and Photonics, 9908AB (2016).

[11] Mahmoud A, Xu D and Xu L, Optical Design of High Resolution and Shared Aperture Electro-Optical/Infrared Sensor for UAV Remote Sensing Applications, IEEE Geoscience and Remote Sensing Symposium, 2921 (2016).

[12] Dmitry Strelnikov, Bastian Kern, Christoph Sürgers and Manfred M. Kappes, Review of Scientific Instruments **88**, 023118 (2017).

[13] Li Yan-jie, Jin Guang, Zhang Yuan and Kong Lin, Chinese Optics **8**, 220 (2015). (in Chinese)

[14] Han Kun-ye, Yang Zi-jian, Chang Wei-jun, Xu Ke, Kang Wenli and Zhang Xuan zhi, Proc. SPIE **9449**, 94492A (2015) .

[15] Wei Bing-xin, Fire Control and Command Control **4**, 55 (1978). (in Chinese)

[16] Wang Zi-chen, Wang Yong-yang, Dai Ming, Zhang Yu-peng and Wang Dong-he, Journal of Optoelectronics·Laser **25**, 317 (2014). (in Chinese)